Acta Crystallographica Section D
**Biological Crystallography**
ISSN 0907-4449

# The structure of human aldose reductase bound to the inhibitor IDD384

**Vito Calderone,[a] Bernard Chevrier,[a] Michael Van Zandt,[b] Valérie Lamour,[a] Eduardo Howard,[a] Arnaud Poterszman,[a] Patrick Barth,[c] André Mitschler,[a] Jianhui Lu,[b] Dushan M. Dvornik,[b] Gerhard Klebe,[d] Oliver Kraemer,[d] Allan R. Moorman,[b] Dino Moras[a] and Alberto Podjarny[a]***

[a]UPR de Biologie Structurale 9004, IGBMC, CNRS/INSERM/ULP, 1 Rue Laurent Fries, BP 163, 67404 Illkirch, France, [b]Institutes for Diabetes Discovery, 23 Business Drive, Branford, CT, USA, [c]Laboratoire de Chimie Organique Biologique, Institut de Chimie, Université Louis Pasteur, 1 Rue Blaise Pascal, 67008 Strasbourg CEDEX, France, and [d]IPC, University of Marburg, Marbacher Weg 6, 35032 Marburg, Germany

Correspondence e-mail: podjarny@igbmc.u-strasbg.fr

Received 18 August 1999
Accepted 8 February 2000

**PDB References:** Human aldose reductase–IDD384, 1el3; porcine aldose reductase–IDD384, 1ek0.

The crystallographic structure of the complex between human aldose reductase (AR2) and one of its inhibitors, IDD384, has been solved at 1.7 Å resolution from crystals obtained at pH 5.0. This structure shows that the binding of the inhibitor's hydrophilic head to the catalytic residues Tyr48 and His110 differs from that found previously with porcine AR2. The difference is attributed to a change in the protonation state of the inhibitor ($pK_a = 4.52$) when soaked with crystals of human (at pH 5.0) or pig lens AR2 (at pH 6.2). This work demonstrates how strongly the detailed binding of the inhibitor's polar head depends on its protonation state.

## 1. Introduction

Aldose reductase (AR2) is implicated in the first step of the sorbitol pathway and is one of the most thoroughly studied aldo–keto reductases owing to its putative involvement in the pathogenesis of diabetic complications (Gonen & Dvornik, 1995). The presence of AR2 in tissues susceptible to diabetic complications has led to the hypothesis that the flow of excess glucose through the sorbitol pathway initiates a continuum of biochemical, functional and early structural abnormalities that can progress to advanced lesions. The fact that increased AR2 activity acts as a trigger of this cascade of abnormalities rests on the evidence that in animal models of diabetic hyperglycaemia, the development of such abnormalities can be prevented by inhibiting AR2, without affecting the elevated glucose concentrations (Dvornik, 1994). The search and development of AR2 inhibitors (ARIs) for the pharmacotherapy of diabetic complications underscored the critical importance of the chemical structure (Dvornik, 1994) because it determines both a compound's ability to inhibit AR2 and its (tissular) pharmacokinetics (Dvornik *et al.*, 1988). All that has been said so far confirms the crucial importance of studying and understanding in depth the interaction between ARIs and AR2 with the aim of designing more potent and specific drugs against diabetic complications.

The crystallographic structures of AR2 and AR2–ARI complexes that have been solved so far have both characterized the main features of the active site and identified the protein residues that are critical for the interaction between the enzyme and its inhibitors. Some examples are the structure determination of native apo-enzyme from pig lens (Rondeau *et al.*, 1992), the native human holo-enzyme (Wilson *et al.*, 1993), the Tyr48His mutation of the human enzyme (Bohren *et al.*, 1994), the native holo-enzyme from pig lens (Tete-Favier *et al.*, 1994), the complexes of the holo-enzyme from pig lens

© 2000 International Union of Crystallography
Printed in Denmark – all rights reserved

with the inhibitors sorbinil and tolrestat (Urzhumtsev *et al.*, 1997), the comparison of the active sites of aldose and aldehyde reductase (El-Kabbani *et al.*, 1998) and the study of several inhibitor complexes by X-ray crystallography and mass spectrometry (Rogniaux *et al.*, 1999).

The inhibitor IDD384 has been prepared as a structural variation of the ARI ZD-5522 (Cook *et al.*, 1995) by replacing its acidic pharmacophore, sulfonyl-nitromethane, with a sulfonyl-glycine moiety. ARIs containing a sulfonyl-glycine group have been reported previously (*e.g.* DeRuiter & Mayfield, 1990). The previously determined structure of the porcine AR2–IDD384 complex (Rogniaux *et al.*, 1999) has confirmed the features of the recognition of AR2–ARI complexes. The main structural features of IDD384 are its polar head and hydrophobic ring system (Fig. 1). While the hydrophobic moiety interacts with the hydrophobic environment of the active-site cleft, the hydrophilic head interacts with protein residues that are essential for catalysis. As shown by the crystal structures, the active-site residues involved in inhibitor binding are Tyr48, His110 and Trp111, mainly through hydrogen bonds. Recognition, therefore, depends on the inhibitor's protonation state. As a part of our investigations of inhibitor–enzyme complexes, we report here on the interaction of the ARI IDD384 with human AR2.

## 2. Materials and methods

### 2.1. Overproduction and purification of recombinant human AR2

The open reading frame of the human AR2 gene (Accession GenBank/EMBL Data Bank number J05017) was amplified by the polymerase chain reaction from its cDNA and cloned into the T7 RNA polymerase-based vector pET15b (Novagen). Expression of the $(His)_6$-human AR2 in *Escherichia coli* strain BL21(DE3) (Novagen) was induced by isopropyl-$\beta$-D-thiogalactoside (Euromedex) during a 3 h culture at 310 K. The pellet from a 4 l culture was disrupted by sonication and centrifuged. The supernatant was applied to a Talon metal-affinity column (Clontech). After thrombin cleavage of the hexahistidine extension, the detagged protein was then loaded on a DEAE Sephadex A-50 column (Pharmacia) and eluted with an NaCl gradient.

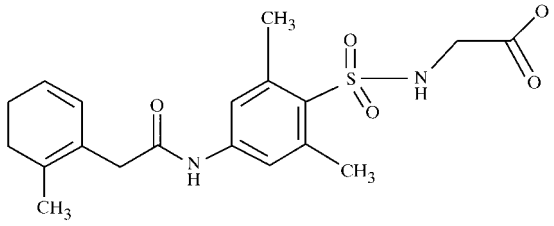

**Figure 1**
Two-dimensional formula for the inhibitor IDD384 which is the subject of the present study. Note that the inhibitor has a hydrophilic head, notably containing C═O groups, and a hydrophobic ring system.

**Table 1**
Data-collection and refinement statistics of the complex of IDD384 with human AR2.

| | |
|---|---|
| Data collection and processing | |
| Unit-cell parameters | |
| $a, b, c$ (Å) | 49.9, 67.2, 47.7 |
| $\alpha, \beta, \gamma$ (°) | 90, 92.5, 90 |
| Diffraction data | |
| $d_{min}$ (A) | 1.7 |
| Unique reflections | 33072 |
| $R_{sym}$ (overall) (%) | 4.7 |
| $R_{sym}$ (1.76–1.7 Å) (%) | 17.0 |
| Completeness (overall) (%) | 95.5 |
| Completeness (1.76–1.7 Å) (%) | 80.0 |
| Redundancy (overall) | 1.5 |
| Redundancy (1.76–1.7 Å) | 1.4 |
| $I/\sigma(I)$ (overall) | 12.0 |
| $I/\sigma(I)$ (1.76–1.7 Å) | 5.4 |
| Rigid-body refinement | |
| Resolution (Å) | 8.0–3.0 |
| $R_{cryst}$ (%) | 20.0 |
| Refinement | |
| Resolution (Å) | 8.0–1.7 |
| Reflections used [$F > 2\sigma(F)$] | 32736 |
| $R_{cryst}/R_{free}$ (%) | 16.5/19.2 |
| $R_{cryst}/R_{free}$ (1.76–1.7 Å) (%) | 21.4/22.5 |
| Final model | |
| Protein residues | 316 |
| Coenzyme | 1 |
| Inhibitor | 1 |
| Water molecules | 239 |
| R.m.s. deviations | |
| Bonds (Å) | 0.006 |
| Angles (Å) | 1.45 |
| Dihedrals (Å) | 25.78 |
| Ramachandran plot | |
| Residues in most favoured regions (%) | 90.3 |
| Residues in additional allowed region (%) | 9.7 |
| Mean $B$ factor (Å$^2$) | |
| Protein | 15.5 |
| $NADP^+$ | 8.8 |
| Ordered IDD384 | 32.3 |

### 2.2. Crystallization trials and preliminary crystallographic analysis

All trials were carried out in Linbro 24-well tissue-culture plates (Flow Laboratories) using the hanging-drop vapour-diffusion method. The enzyme was dialyzed against 50 m*M* ammonium citrate pH 5.0. The drops, of final volume 12 µl, contained 15 mg ml$^{-1}$ human AR2 with two equivalents $NADP^+$ (Sigma) and 5% PEG 6000; they were equilibrated against a well containing 120 m*M* ammonium citrate pH 5.0, 20% PEG 6000 and the same concentration of $NADP^+$ as above. Crystals were grown at 277 K and reached dimensions of 0.5 × 0.4 × 0.4 mm.

### 2.3. Soaking with the inhibitor

Crystals of the AR2–IDD384 complex were obtained by soaking the native crystals with a solution containing 2 mg ml$^{-1}$ of inhibitor dissolved in the mother liquor containing 120 m*M* ammonium citrate pH 5.0 and 25% PEG 6000. The soaking time was three weeks.

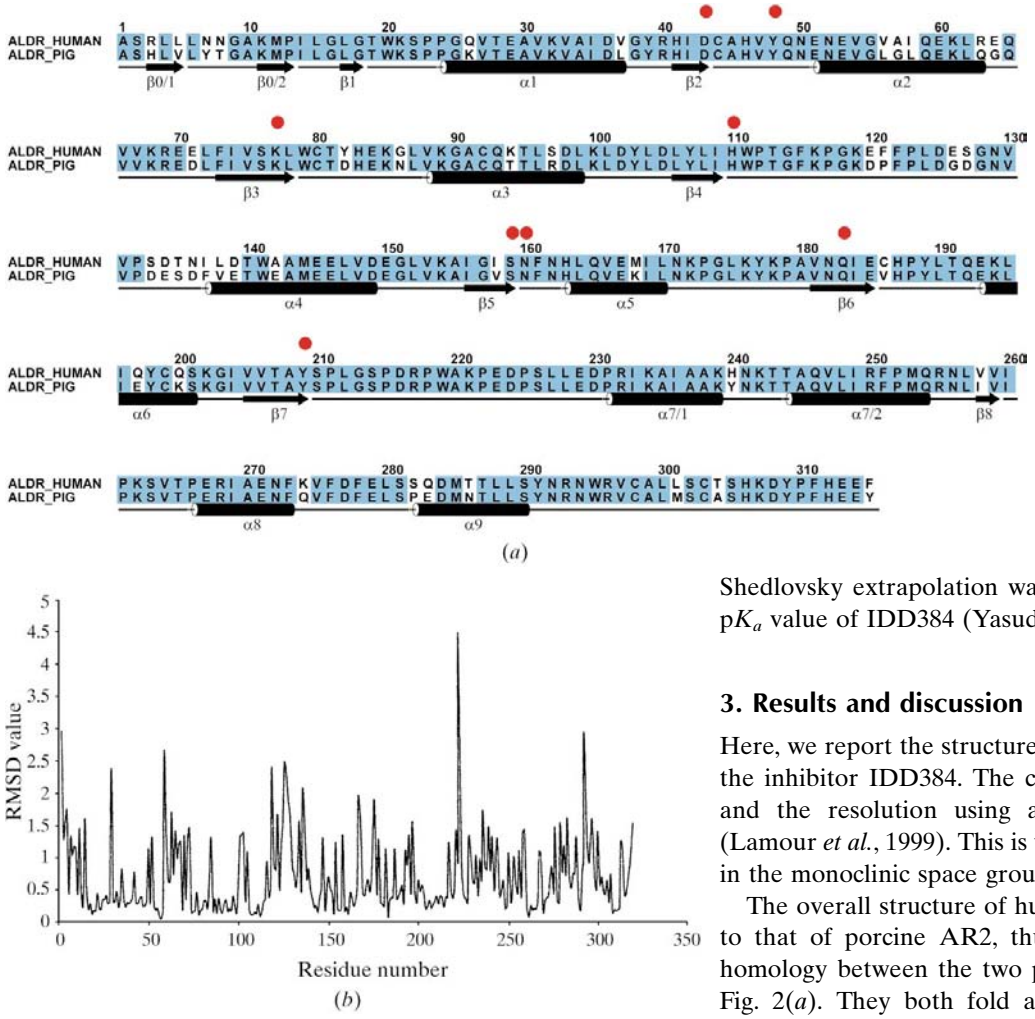


**Figure 2**
(*a*) Sequence alignment between human and porcine AR2, showing the very high homology in the primary structure. Identical residues are highlighted in light blue. The red dots correspond to the conserved residues forming the hydrophilic network around the NADP$^+$. The helices ($\alpha$) and sheets ($\beta$) are marked below the sequence; those numbered 1–8 correspond to the TIM barrel. (*b*) Plot of the r.m.s. deviations between the C atoms of the human and porcine structures (the last two residues are NADP$^+$ and IDD384).

### 2.4. Data collection and refinement

The diffraction analysis was performed using a rotating-anode laboratory source and an image plate; the data was treated with the *HKL* package (Otwinowski & Minor, 1997). The inhibitor-soaked crystals diffracted to 1.7 Å and were isomorphous to the native crystals (Table 1).

The native structure was used as a model for molecular replacement; after a rigid-body minimization, the inhibitor was placed in the electron density shown by a Fourier difference map. The model of the complex was used as the starting point for the refinement, which included a rigid-body refinement step, a slow-cooling step, a Powell minimization and a temperature-factor refinement. Water molecules were then placed in a difference map and minimization was performed as above without putting restraints on the water molecules; bulk-solvent correction was also applied. The programs *O* (Jones *et al.*, 1991) and *X-PLOR* (Brünger, 1992) were used for model building and refinement.

### 2.5. Titration of the inhibitor

The inhibitor IDD384 was titrated potentiometrically with a pH-sensitive electrode using the PCA 101 device from Sirius Analytical Instruments, England, in mixtures of water and dioxane; the Yasuda–Shedlovsky extrapolation was used to calculate the aqueous p$K_a$ value of IDD384 (Yasuda, 1959; Shedlovsky, 1962).

## 3. Results and discussion

Here, we report the structure of human AR2 in complex with the inhibitor IDD384. The crystals were obtained at pH 5.0 and the resolution using a laboratory source was 1.7 Å (Lamour *et al.*, 1999). This is the first structure of human AR2 in the monoclinic space group $P2_1$.

The overall structure of human AR2 is highly homologous to that of porcine AR2, thus reflecting the high sequence homology between the two proteins, shown schematically in Fig. 2(*a*). They both fold as a $(\beta/\alpha)_8$ barrel and the high structural homology between the two $\beta$-barrels corresponds to the regions of low r.m.s. deviation (Fig. 2*b*). The coenzyme NADP$^+$ lies on the binding site at the top of the barrel and the active site lies at the bottom of a deep hydrophobic pocket. In both structures, conformational changes arising from the binding of the coenzyme affect the (same) loop that covers the coenzyme.

As reported previously (Urzhumtsev *et al.*, 1997), all effective ARIs have a polar head and a hydrophobic ring system and bind to the active site with the polar head placed close to the coenzyme. The hydrophilic head of the inhibitor IDD384 could be unambiguously positioned in the density map (Fig. 3*a*). In the active site, several residues are totally conserved, *i.e.* Asp43, Tyr48, Lys77, His110, Ser159, Asn160, Gln183 and Tyr209 (Fig. 2*a*), and form a tight network of hydrogen bonds linked to the nicotinamide coenzyme (Fig. 3*b*). As in porcine AR2, the three residues involved in the interaction of human AR2 with the inhibitor are Tyr48, His110 and Trp111 (Fig. 4).

The only significant difference between the two complexes is in the binding of IDD384 at the active site of the human AR2. While in human AR2 both carboxyl O atoms of IDD384 are at hydrogen-bonding distance from the hydroxyl group of Tyr48, in porcine AR2 one of the two carboxyl O atoms is far away from Tyr48 (Fig. 4). This suggests that the inhibitor

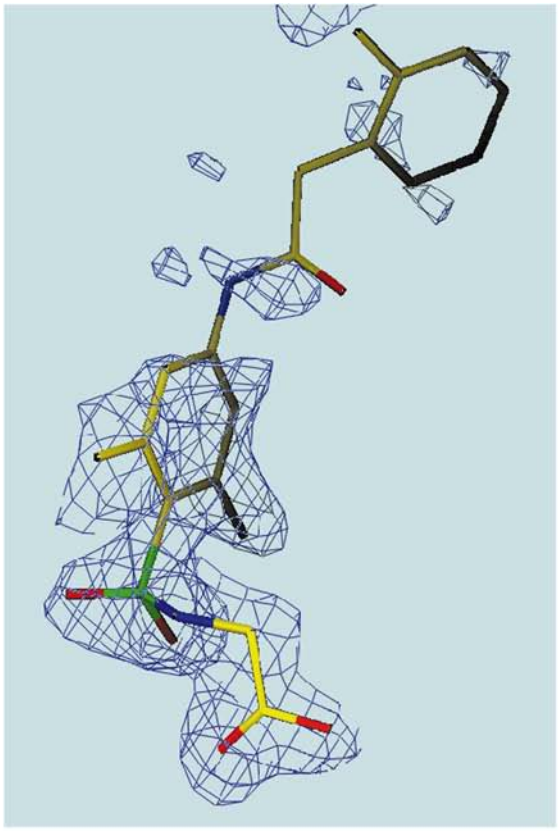

(*a*)

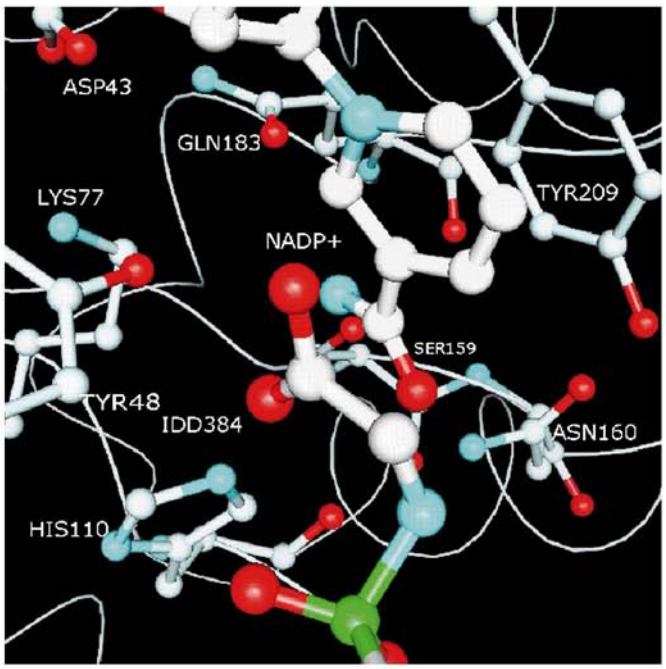


(*b*)

**Figure 3**
(*a*) Electron-density map ($2F_o - F_c$, 1.7 Å resolution, $1\sigma$ contours) showing the density corresponding to the inhibitor bound at the active-site cleft of human AR2. Note that the ordered part of the inhibitor is that in contact with the active-site cleft. (*b*) A detailed view showing the inhibitor and the $NADP^+$ in the human active site with the the residues making the hydrophilic network around the nicotinamide ring. Note the positions of Tyr48 and His110 near the O atom of the inhibitor.

IDD384 adopts a different protonation state in each complex. We assumed that the difference between the human and porcine complex arises from the difference in pH at which the crystals of complexes with IDD384 have been obtained, *i.e.* at 6.2 for porcine and 5.0 for human AR2.

We determined the $pK_a$ constant for IDD384 using the Yasuda–Shedlovsky extrapolation (Fig. 5). Given the resulting $pK_a$ value of 4.52, an appreciable portion of the inhibitor would have been protonated in the complex with human AR2 at pH 5.0 and could be the one that is preferably bound. The analysis of the distances between the hydrophilic head of IDD384 and the protein in the porcine and human enzymes, shown in Fig. 4 (blue C atoms for porcine, white C atoms for human), is consistent with the hypothesis of a protonated inhibitor at pH 5. In the human enzyme, the distances between both O atoms of the inhibitor and Tyr48 are around 2.7 Å, showing strong hydrogen bonds in which one proton has to come from the inhibitor. On the other hand, in the porcine enzyme, one O atom is very strongly bound with short hydrogen bonds around 2.45 Å, while the other is at a longer distance (3.14 Å), indicating the absence of a proton.

## 4. Conclusions

The crystallographic structure of the complex between human AR2 and one of its inhibitors, IDD384, has been solved at 1.7 Å resolution from crystals obtained at pH 5.0. This structure has been compared with that of the complex between IDD384 and porcine AR2 solved at 2.2 Å resolution from crystals grown at pH 6.2. We have found that IDD384 is bound

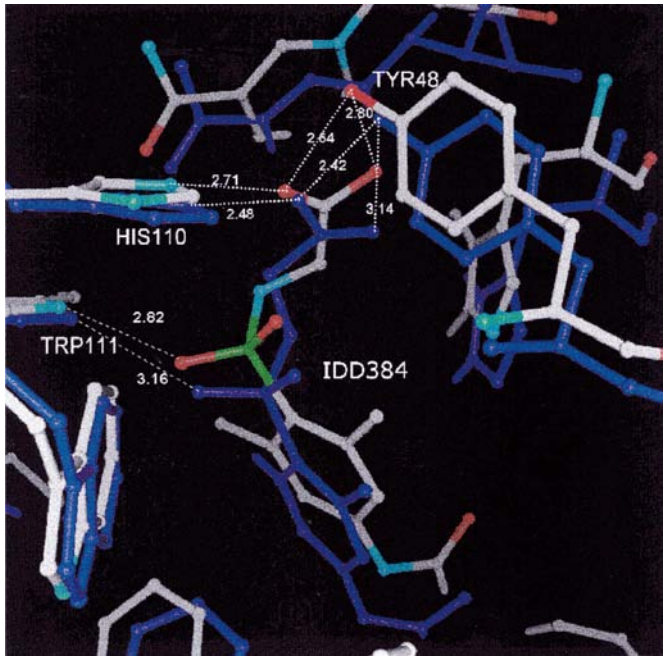


**Figure 4**
Superimposition of IDD384 in complex with human AR2 with IDD384 in complex with the porcine enzyme (blue). Hydrogen bonds with the two catalytic residues Tyr48 and His110 are shown as white dotted lines.

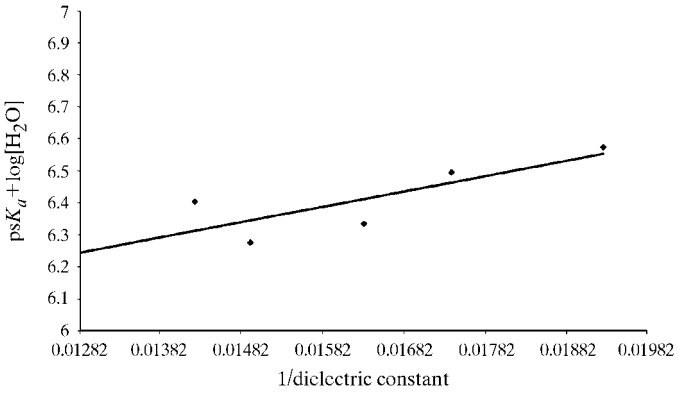


**Figure 5**
Yasuda–Shedlovsky plot for the inhibitor IDD384. The titrations were carried out in the pH range 2.5–11.0 for different dioxane/water mixtures with 0.15 *M* KCl; thus, only the p$K_a$ of the carboxylic acid was determined. The Yasuda–Shedlovsky extrapolation was used to calculate the aqueous p$K_a$ of IDD384 to be 4.52. The dielectric constant of pure water at 298 K is 78.3; hence, 1/dielectric constant = 0.012.

differently by human than by porcine AR2 because of an additional hydrogen bond between one of the inhibitor's carboxylic O atoms and the hydroxyl group of Tyr48. We attribute the observed difference in binding to the difference in pH at which the complexes with IDD384 (p$K_a$ = 4.52) have been obtained, *i.e.* at pH 5.0 for human and at pH 6.2 for porcine AR2: at pH 5, a significant portion of the inhibitor would be protonated and preferred for binding by the enzyme owing to the additional hydrogen-bonding energy. This work demonstrates how strongly the detailed binding of the inhibitor's polar head depends on its protonation state. It implies that ongoing efforts of computational modelling of new inhibitor molecules need to consider the p$K_a$ of inhibitors and their possible protonation state at physiological pH.

We would like to thank Frank Dullweber (University of Marburg) for his assistance in determining the p$K_a$ values. This work was supported by the Centre National de la Recherche Scientifique (CNRS) through the UPR 9004 and by the collaborative project 5834 CNRS-CONICET, by the Institut National de la Santé et de la Recherche Médicale and the Hôpital Universitaire de Strasbourg (HUS) and by the Institute of Diabetics Discovery Industries through a contract with the CNRS.

## References

Bohren, K. M., Grimshaw, C. E., Lai, C. J., Harrison, D. H., Ringe, D., Petsko, G. A. & Gabbay, K. H. (1994). *Biochemistry*, **33**, 2021–2032.
Brünger, A. T. (1992). *X-PLOR. A System for Crystallography and NMR.* New Haven, CT, USA: Yale University Press.
Cook, P. N., Ward, W. H., Petrash, J. M., Mirrlees, D. J., Sennitt, C. M., Carey, F., Preston, J., Brittain, D. R., Tuffin, D. P. & Howe, R. (1995). *Biochem. Pharmacol.* **49**, 1043–1049.
DeRuiter, J. & Mayfield, C. A. (1990). *Biochem. Pharmacol.* **40**, 2219–2226.
Dvornik, D. (1994). *Design of Enzyme Inhibitors as Drugs*, Vol. 2, pp. 710–738. Oxford University Press.
Dvornik, D., Millen, J., Hicks, D., Cayen, M. & Sredy, J. (1988). *The Polyol Pathway and its Role in Diabetic Complications*, edited by H. Sakamoto, J. H. Kinoshita, P. F. Kador & H. Hotta, pp. 61–71. Amsterdam: Elsevier.
El-Kabbani, O., Wilson, D. K., Petrash, J. M. & Quiocho, F. A. (1998). *Mol. Vis.* **4**, 19–25.
Gonen, A. & Dvornik, D. (1995). *Clinical Science of Diabetes*, edited by D. E. Robbins & D. Leslie, pp. 313–330. Cambridge University Press.
Jones, T. A., Zou, J. Y., Cowan, S. W. & Kjeldgaard, M. O. (1991). *Acta Cryst.* A**47**, 110–119.
Lamour, V., Barth, P., Rogniaux, H., Poterszman, A., Howard, E., Mitschler, A., Vandorsselaer, A., Podjarny, A. & Moras, D. (1999). *Acta Cryst.* D**55**, 721–723.
Otwinowski, Z. & Minor, W. (1997). *Methods Enzymol.* **276**, 307–326.
Rogniaux, H., Barbanton, J., Barth, P., Chevrier, B., Howard, E., Mitschler, A., Potier, N., Urzhumtseva, L., van Zandt, M., Biellmann, J.-F, Moras, D., Van Dorsselaer, A. & Podjarny, A. (1999). *J. Am. Soc. Mass Spectrom.* **10**, 635–647.
Rondeau, J. M., Tete-Favier, F., Podjarny, A. D., Reymann, J. M., Barth, P., Biellmann, J.-F. & Moras, D. (1992). *Nature (London)*, **355**, 469–472.
Shedlovsky, T. (1962). *Electrolytes*, edited by B. Pesce, pp. 146–151. New York: Pergamon Press.
Tete-Favier, F., Barth, P., Mitschler, A., Podjarny, A. D., Rondeau, J. M., Urzhumtsev, A., Biellmann, J.-F. & Moras, D. (1994). *Reports of the 13th Symposium of Medicinal Chemistry*, edited by J. C. Muller, pp. 589–603. Paris: Elsevier.
Urzhumtsev, A., Tete-Favier, F., Mitschler, A., Barbanton, J., Barth, P., Urzhumtseva, L., Biellmann, J.-F., Podjarny, A. D. & Moras, D. (1997). *Structure*, **5**, 601–612.
Wilson, D. K., Tarle, I., Petrash, J. M. & Quiocho, F. A. (1993). *Proc. Natl Acad. Sci. USA*, **90**, 9847–9851.
Yasuda, U. (1959). *Bull. Chem. Soc. Jpn*, **32**, 429–432.